Organic Electronics 14 (2013) 3052–3060

Contents lists available at ScienceDirect

Organic Electronics

journal homepage: www.elsevier.com/locate/orgel

Soldering of solution-processed organic vertical transistor and light-emitting diode on separate glass substrates by tin micro-balls

Yu-Hsin Lin [a], Yu-Fan Chang [b], Hsin-Fei Meng [a,*], Hsiao-Wen Zan [b,*], Wensyang Hsu [c], Chao-Hsuan Chen [b]

[a] Institute of Physics, National Chiao Tung University, 1001, Ta-Hsueh Rd, Hsinchu 300, Taiwan
[b] Department of Photonics and Institute of Electro-Optical Engineering, National Chiao Tung University, 1001, Ta-Hsueh Rd, Hsinchu 300, Taiwan
[c] Department of Mechanical Engineering, National Chiao Tung University, 1001, Ta-Hsueh Rd, Hsinchu 300, Taiwan

ARTICLE INFO

Article history:
Received 14 April 2013
Received in revised form 2 July 2013
Accepted 3 July 2013
Available online 30 July 2013

Keywords:
Organic vertical transistor
Soldering
Tin micro-balls
Organic light-emitting diode
Space-charge-limited transistor

ABSTRACT

The vertical organic space-charge-limited transistor made of P3HT and small-molecule phosphorescent organic light-emitting diode (OLED) are made on two separate glass substrate by blade coating, then soldered vertically together by tin balls with 40 μm diameter. The soldering is done by hot wind of 150 °C for 5 min Contact resistance is only 10 Ω. The vertical transistor is annealed at 150 °C for 5 min before soldering to enhance the output current up to 25 mA/cm^2 and give high thermal stability. Both OLED and the annealed vertical transistor are not affected by the soldering process. The vertical transistor has 1/4 of the OLED area and turns on the bottom-emission white OLED up to 300 cd/m^2 and orange OLED up to 600 cd/m^2. The entire operation is within 8 V. OLED and transistor array can therefore be made on separate glass substrates then soldered together to form the display.

1. Introduction

Active-matrix organic light-emitting diode (AMOLED) is an emerging technology for display. It has the advantages of good color quality, high response speed, and low thickness compared with the conventional liquid crystal display. A variety of vacuum-processed transistor backplanes are used for the pixel driving circuit of AMOLED including amorphous silicon, poly-crystalline silicon, oxide semiconductor like IGZO [1–3], and organic field-effect transistors [4,5]. The OLED and the transistor are usually fabricated on the same glass substrates [1–5]. The aperture ratio is limited by the pixel area occupied by the transistors, therefore the OLED can only have top emission [3]. In top-emission OLED the device structure is usually more complicated and the view angle is narrow because of the optical cavity effect. Furthermore, the efficiency of white OLED is greatly reduced in the top-emission structure relative to the conventional bottom emission structure. This is because only part of the broad white emission spectrum matches the cavity resonance wavelength. For large area AMOLED white OLED in combination with color filter has the great advantage that no patterning is necessary for all the organic semiconductor layers. Indeed the difficulty related to the shadow mask patterning for individual red, green, and blue OLED increases dramatically with display size. If the OLED and the transistor can be fabricated on separate substrates and connected together afterwards, OLED with convenient bottom emission structure and white OLED without any patterning can be used in AMOLED. In addition, such afterward connection avoids the potential conflict in

* Corresponding authors. Tel.: +886 35731955 (H.-F. Meng).
E-mail addresses: meng@mail.nctu.edu.tw (H.-F. Meng), hsiaowen@mail.nctu.edu.tw (H.-W. Zan).

1566-1199/$ - see front matter © 2013 Elsevier B.V. All rights reserved.
http://dx.doi.org/10.1016/j.orgel.2013.07.005

OLED and transistor process temperature and the devices can be individually optimized. Connection of OLED and amorphous-silicon on separate substrates are reported by direct hard metal contact [6]. Without any soldering such contact gives high contact resistance [6], and poor uniformity is expected due to the inevitable random air gap up to 10 μm between the glass substrates resulting from the glass unevenness. Large-area AMOLED will become practical only if both OLED and the transistor can be solution-processed without patterning, and they can be reliably soldered together after separated optimized fabrication.

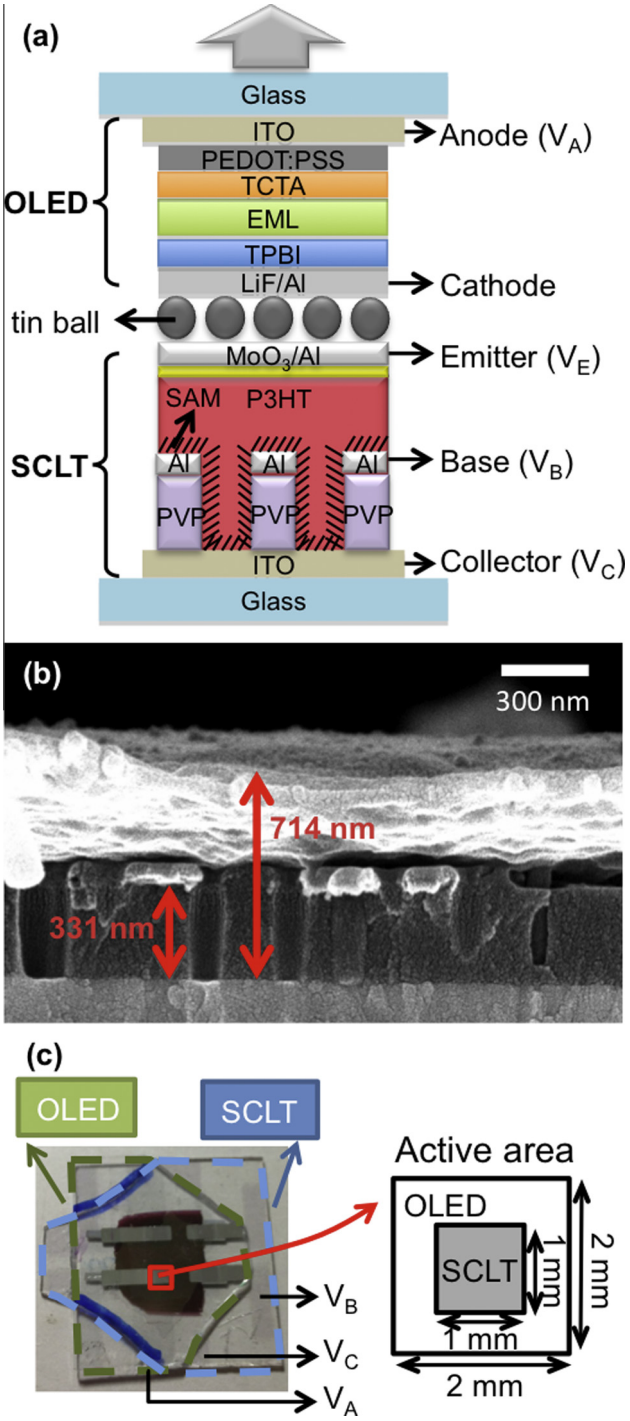

Fig. 1. (a) Schematic diagram of OLED and SCLT after soldering by tin balls. The device structure consists of two separate glass substrate, i.e., the bottom substrate involving SCLT with SAM treatment and the top substrate involving bottom-emission white OLED. (b) The SEM cross-section image of SCLT structure. (c) The active areas and relative position of the two devices.

In this work we connect the solution-processed vertical organic transistor, the space-charge-limited transistor (SCLT), and the phosphorescent white OLED on separate glass substrates using tin balls with 40 μm diameter as solder. Such diameter is sure to fill any air gap. SCLT is chosen because of its high current output and low operation voltage [7] which are necessary for OLED driving. Both the SCLT and the OLED are made by blade coating, which is shown to be suitable for low-cost large-area fabrication [8–12]. Tin balls have the low melting point of 139 °C and they can easily melted by applying a hot wind shortly. The SCLT is post-annealed to reach a stable characteristic before soldering. It is found that the performance of SCLT and OLED are not compromised by the hot wind. Low contact resistance of 10 Ω is achieved by such soldering. The luminance of the white OLED can be switched from off to a typical value of 300 cd/m^2 for display by the SCLT with only 1/4 of the area. The two glasses also readily encapsulate the devices in between. The success of the soldering opens the new strategy of large-area solution-processed AMOLED by the face-to-face lamination of white OLED array plane and the transistor backplane after individual optimized fabrication.

2. Experimental

2.1. Individual space-charge-limited transistor and OLED by blade coating

The vertical space-charge-limited transistor (SCLT) depicted in Fig. 1a is conceptually a solid-state vacuum tube. The vertical hole current in the organic semiconductor is modulated by the metallic grid base. The transistor operation principle and the device properties have been described elsewhere [7,13]. It is previously shown to achieve the output current density of 50 mA/cm^2 [7] which is larger than the typical current density for high-efficiency phosphorescent OLED. The SCLT cross section is shown in Fig. 1a. In this work the poly(4-vinylphenol) (PVP) insulator thickness is 331 nm and the total semiconductor thickness is 714 nm as indicated in Fig. 1b. The poly(3-hexylthiophene) (P3HT) is used as the active organic semiconductor. The vertical channel side wall is treated by the self-assembled monolayer (SAM) of octadecyltrichlorosilane (OTS-18) in order to enhance the P3HT filling into the channel [7]. The SCLT structure is shown in the electro-scanning microscopy (SEM) images in Fig. 1b. The OLED on a separate

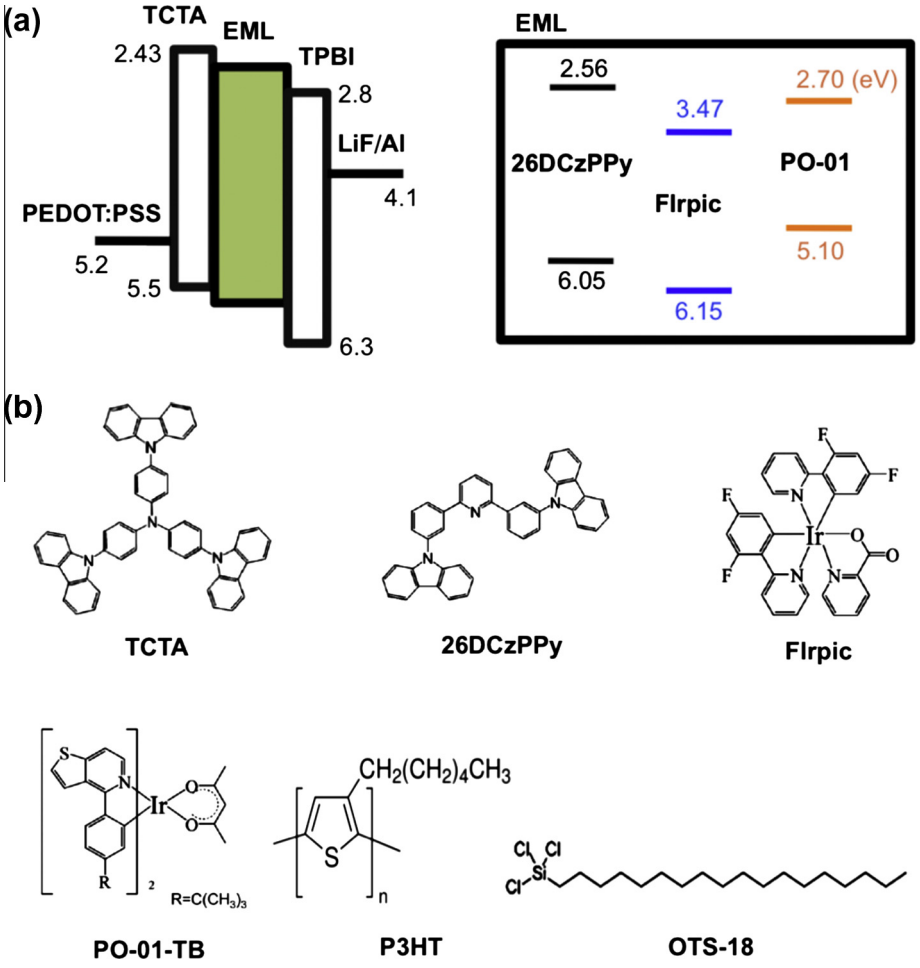

Fig. 2. (a) The energy levels of white OLED. (b) The chemical structures of the used materials.

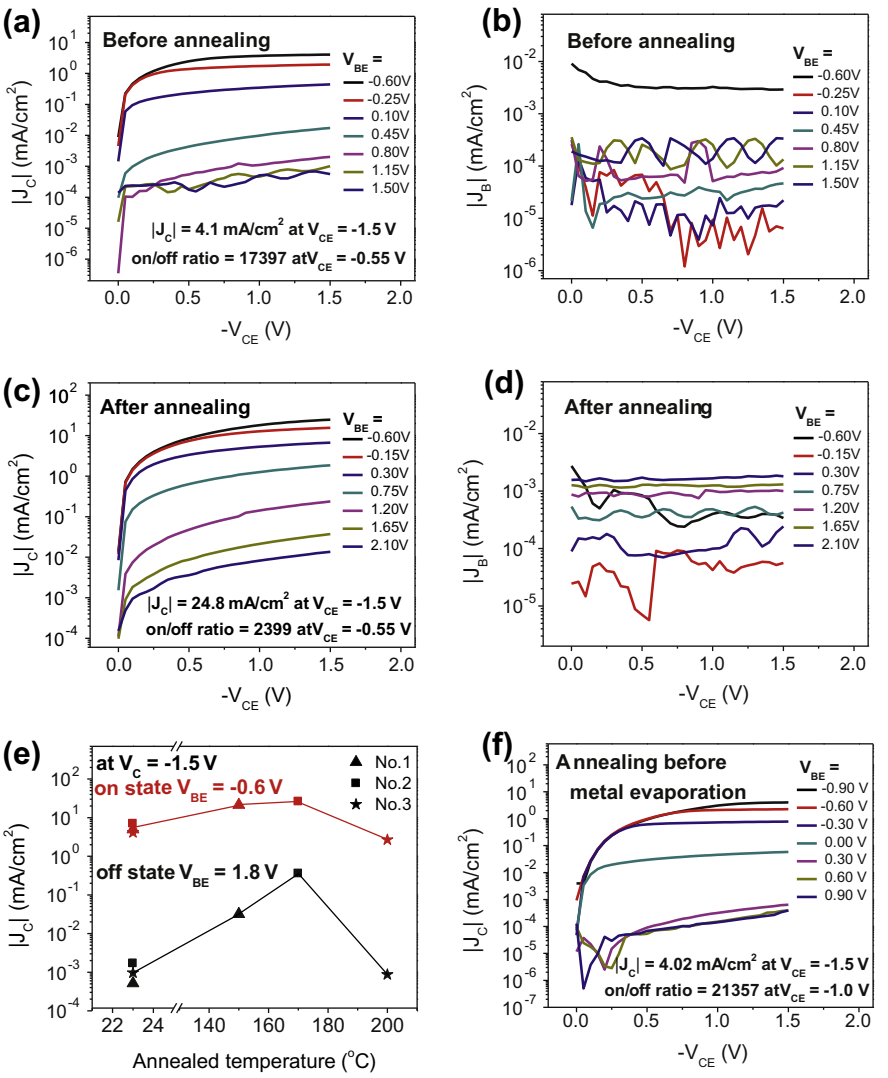

Fig. 3. (a) The J_C–V_{CE} curves and (b) base leakage current density J_B of SCLT before post-annealing at different V_{BE}. (c) The J_C–V_{CE} curves and (d) base leakage current density J_B of SCLT after post-annealing at different V_{BE}. (e) The on-current and off-current of J_C measured at V_C = −1.5 V of various SCLTs No. 1–3 before and after annealing separately at 150 °C, 170 °C and 200 °C for 5 min (the line drawn for the eyes). (f) The J_C–V_{CE} curves of SCLT annealed at 150 °C for 5 min before MoO_3/Al evaporation at different V_{BE}.

glass substrate is also shown in Fig. 1a. The LiF/Al cathode is to be connected with the Al emitter of SCLT by soldering below. Multi-layer phosphorescent OLED by small molecules are fabricated by blade coating as described previously [10,11]. The OLED is 2 mm by 2 mm and SCLT is 1 mm by 1 mm. Note that SCLT has high enough current density to drive OLED with size several times larger. This is important for the complete 2-transistor 1 capacitor (2T1C) pixel circuit. The relative position of the two devices is shown in the picture of Fig. 1c. The energy levels and chemical structures of some materials are shown in Fig. 2a and b. The device fabrication conditions are given below.

2.2. SCLT fabrication

The SCLT is fabricated on an indium-tin-oxide (ITO) glass substrate. Cross-linkable PVP of 330 nm is spin coated on ITO substrate and annealed at 200 °C for 60 min. Poly (mela-mine-co-formaldehyde) methylated is utilized as a cross-linking agent for PVP. After modifying the PVP surface energy by coating a thin P3HT layer, the polystyrene (PS) spheres of 100 nm diameter are adsorbed on the substrate [12]. 40 nm of aluminum is deposited by evaporation as the metal base electrode, the PS spheres are removed by adhesive tape (Scotch, 3 M) and the PVP beneath the Al opening, defined by the PS spheres, is removed by 100 W O_2 plasma. After treating the structure with OTS-18 by immersion for 2 h, it is transferred to the nitrogen glove box and about 700 nm of P3HT is blade coated in chlorobenzene solution then annealed at 200 °C for 10 min. Finally, the MoO_3 (10 nm)/Al (100 nm) collector is evaporated to complete the SCLT with active area as 1 mm^2.

2.3. OLED fabrication

The OLED is also fabricated on the glass substrates with patterned ITO layer. After using UV-ozone treatment, 50 nm hole injection layer of poly-(3,4-ethylenedioxythiophene): poly-(styrenesulfonate) (PEDOT:PSS CLEVIOSTM P VP AI 4083) is spin coated and annealed at 200 °C for 15 min. The substrates are then taken into a nitrogen glove-box. The 30 nm of 4,4′,4″-tris(carbazol-9-yl) triphenylamine (TCTA) used as the hole transporting layer is blade coated with gap of 60 m and annealed at 100 °C for 10 min in vacuum environment (10^{-3} torr) to remove the residual solvent. For emission layer, two chlorobenzene solutions with 2,6-bis (3-(9H-carbazol-9-yl)phenyl) pyridine (26DCzppy) to bis (3,5-difluoro-2-(2-pyridyl) phenyl-(2-carboxypyridyl)I ridium(III) (FIrpic) weight ratio of 89: 11, 26DCzppy to iridium (III)bis (4-(4-t-butylphenyl) thieno[3,2-c]pyridinato-N,C2′) acetylacetonate (PO-01-TB) weight ratio of 89:11 are separately prepared and mixed with the prescribed weight ratio of 30:1. The solution of 30 μl is delivered in front of the blade by a pipette, the blade with a 60 μm gap is then moved at 200 mm/s on a hot plate (at 80 °C). The emission layer with thickness 40 nm is then baked for 80 °C for 10 min in vacuum environment (10^{-3} torr). Then, the 50 nm of electron transporting layer 2,2′,2″- (1,3,5-benzinetriyl)-tris (1-phenyl-1-H-benzimidazole) (TPBI) is blade coated with methanol solution of 50 μl at 450 mm/s. The LiF (0.8 nm)/Al (100 nm) cathode is evaporated to complete the OLED with active area as 4 mm^2.

3. Results and discussions

3.1. Effect of post annealing for vertical transistor

The SCLT needs to endure the heating during soldering to be discussed below. The melting temperature of tin ball is 139 °C, so after the MoO_3/Al emitter evaporation the SCLT is post-annealed before soldering. In this way the device characteristics is not altered by soldering. Before post-annealing the SCLT performance is shown in Fig. 3a and b. The device has top emitter and bottom collector as shown in Fig. 1a. The collector current density J_C reaches 4 mA/cm^2 at collector voltage V_C of −1.5 V relative to the emitter. The on–off ratio is about 10^4 and the base leakage current density J_B is low as shown in Fig. 3b. After post-annealing to 150 °C the collector current density J_C reaches 24.8 mA/cm^2 at collector voltage V_C of −1.5 V and leakage current density is altered as shown in Fig. 3c and d. The output current density J_C increases after post annealing up to 170 °C as shown in Fig. 3e, then drops at higher temperature. The annealing time is 5 min. Unfortunately the off-current of J_C also increases with annealing temperature up to 170 °C. According to Fig. 3e 150 °C appears to be the optimal temperature, as the on-current is raised and the off-current stays at an acceptable level. Luckily this temperature is just enough to melt the tin balls. The devices No. 1–3 are independent samples with similar initial performance before annealing. Each sample is annealed only once. One possibility for this increase of output current is the improved contact between P3HT and MoO_3/Al top

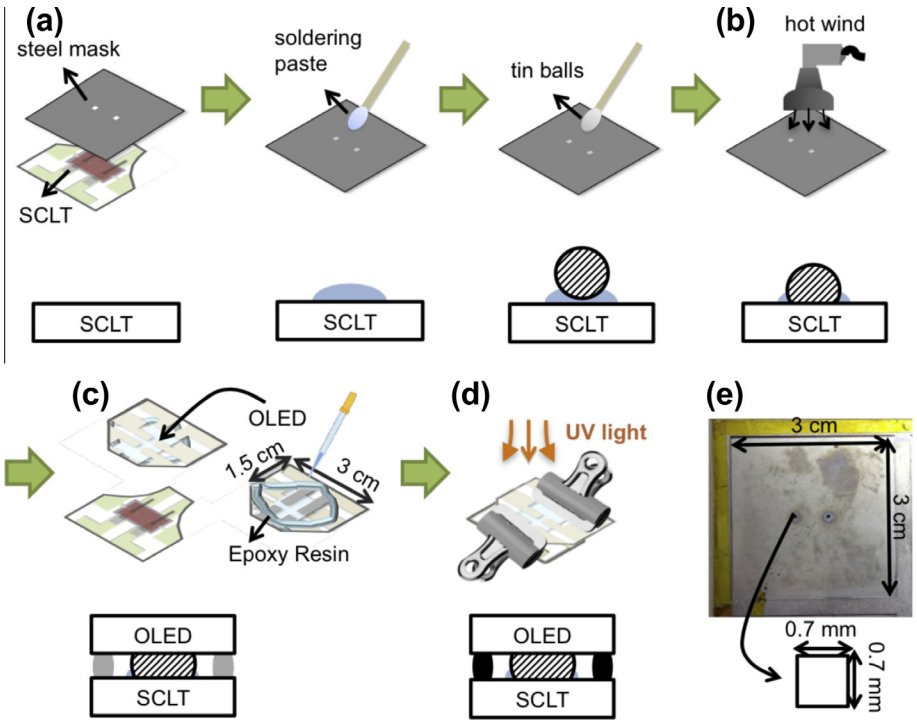

Fig. 4. The process flow chart of soldering SCLT and OLED by tin balls. (a) The planting of tin balls. (b) Melt of tin balls. (c) The nice contact with OLED cathode and SCLT emitter. (d) The devices encapsulated by UV epoxy. (e) The image of stainless steel mask with opening area of 0.7 mm by 0.7 mm.

emitter electrode, such effect of post-annealing on contact has been reported for organic solar cell [14] and field-effect transistor [15]. In order to verify this we study SCLT which is annealed at similar conditions before emitter thermal evaporation. In Fig. 3f it is shown that if the annealing is done before metal evaporation it has no effect on the transistor performance. This is in sharp contrast to the case that annealing is done after metal evaporation, and supports the possibility of metal contact improvement. Another possibility for the output current increase at 150 °C annealing is that the existence of top electrode may hold the morphology change by annealing, as this temperature is marginal for the transformation from fibrils to grains structures [15]. Without the top electrode the thermal-induced grains may disintegrate back to fibrils once the temperature drops. Once the SCLT is post-annealed at 150 °C for 5 min, further long time annealing at this temperature is found to have almost no effect. The device is now stable enough for the subsequent soldering step. When the annealing temperature is raised to 200 °C both the on and off current of the transistor are reduced significantly as shown in Fig. 3e. The P3HT film with granular morphology is reported to have lower mobility than the film with fibular morphology, and 200 °C is well above the transformation critical temperature [15]. The drop in output current with annealing well above 150 °C is therefore probably due to the mobility decrease caused by morphology change.

3.2. Tin ball soldering

The tin balls of 40 μm diameter is from Accurus Scientific Co., Ltd. The exact composition is 42.274% Tin (Sn), 57.7045% Bismuth (Bi), 0.0104% Copper (Cu), 0.0030% Antimony (Sb), 0.0024% Lead (Pb), 0.0023% Silver (Ag), 0.0012% Arsenic (As), 0.0011% Indium (In), 0.0006% Iron (Fe), 0.0002% Aluminum (Al), 0.0001% Zinc (Zn), 0.0001% Cadmium (Cd) and 0.0001% Nickel (Ni). It is to be used to the soldering paste from Taiyo Electric Ind. Co., Ltd. The paste composition is vaseline 80–90 wt.%, zinc chloride 4–6 wt.%, water 2–4 wt.%, paraffin 6–9 wt.% and ammonium chloride 1–3 wt.%. The two edges of the 3 cm by 3 cm glass substrate of SCLT is first cut such that the ITO pad for the OLED glass substrate is not covered after face-to-face

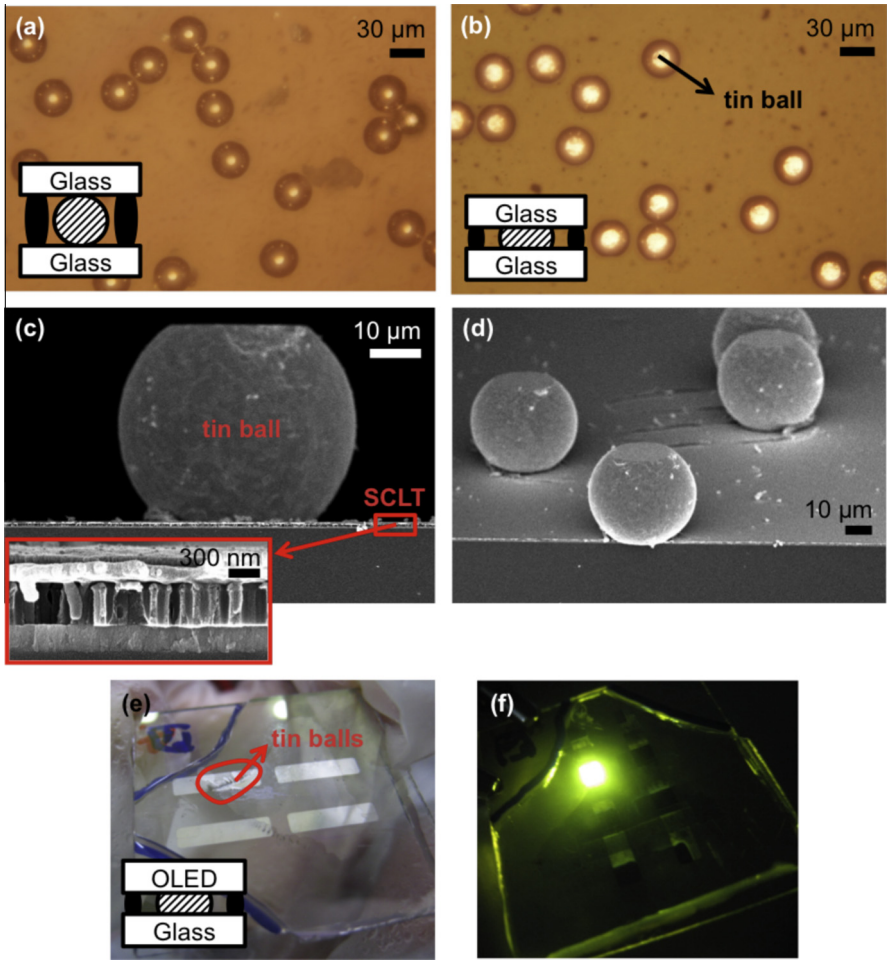

Fig. 5. The optical microscope images of the tin balls placed between two blank glasses (a) without hot wind heating and (b) with hot wind heating at 150 °C for 5 min (c) The SEM cross-section image of the tin balls on SCLT magnified locally. (d) The SEM image of the tin balls on SCLT. (e) The images of device replacing SCLT with glass on the same fabricated process. (f) The image of highly uniform device.

lamination as shown in Fig. 4a. Similarly the two edges of the OLED glass substrate are also cut in order to expose the ITO pad of OLED. A stainless steel mask with opening area of 0.7 mm by 0.7 mm shown in Fig. 4e is used to define the region of soldering paste and tin balls. Both of them are applied by a cotton swab through the opening. The tin balls that are not immobilized by the soldering paste are removed by blowing through the mask. Downward hot wind of 150 °C is then applied for 5 min as shown in Fig. 4b such that the tin balls are melted. In principle bottom heating by hot plate is also possible but it has the problem of slow and non-uniform thermal conductivity through the glass. After hot wind the glass substrate containing the OLED is quickly laminated on top of the SCLT substrate with some pressure. Because of the tin balls are soft before cooling the top and bottom becomes flat as shown in Fig. 4c. Nice contact with the top OLED cathode and the bottom SCLT emitter is formed in this soldering process. The OLED substrate is pre-deposited with UV epoxy such that the devices are automatically encapsulated. Clippers are used to fix the two substrates and UV is applied to cure the epoxy as shown in Fig. 4d. The entire process is done in a nitrogen glove box. In order to verify that proper soldering is achieved, the tin balls are placed between two blank glasses with the same process above. After lamination the two glasses are detached to exam the shape of the tin balls by optical microscope. The results are shown in Fig. 5a and b. Without hot wind heating the tin ball basically keeps a sphere shape, whereas with hot wind heating a significant portion of the sphere becomes flat. The SEM images of the tin balls on SCLT are shown in Fig. 5c and d where the SCLT vertical channels are visible in the local magnification. It is important that the SCLT structure is not crushed by the tin ball pressure during lamination of the two substrates.

The contact resistance of the tin ball soldering can be obtained from the total resistance between the OLED cathode pad to the SCLT emitter pad. The resistances of the contact pads to the device electrodes can be independently measured. The contact resistance is therefore the total resistance subtracted by the two pad-to-electrode resistances. The subtracted value is about 10 Ω. This is far lower than the effective resistance of the SCLT and OLED in the range of MΩ. After soldering, it is necessary to check the potential damages on the device performance by the 150 °C hot wind and the pressure. The OLED emission remains uniform as shown in Fig. 5e and f, implying the absence of crystallization even though the top electron-transport material TPBI has a glass transition temperature of 127 °C below the soldering temperature of 150 °C. As for SCLT, the performances before and after soldering are compared in Fig. 6a and b. It is shown that it is quite stable against temperature once it is post-annealed.

3.3. OLED driven by SCLT after soldering

Combining the low contact resistance and stable device performance of the tin ball soldering, the OLED can be driven by the SCLT in the concept shown in Fig. 1c, where the area of the SCLT is only 1/4 of the OLED area. 3/4 of the area is reserved for the switching transistor and the capacitor in the 2T1C pixel circuit as the entire 2T1C needs to fit within the OLED area. The characteristics of the white OLED is shown in Fig. 7a–d. Low current density is required for such high-efficiency phosphorescent OLED. As discussed above all the semiconductor layers of the OLED and SCLT are deposited by the blade coating method [7,10,11] suitable for large area. After soldering connection there are three external terminals shown in Fig. 8. The collector bias V_C is fixed at zero and the OLED anode bias V_A is fixed at 8 V. The downward current is modulated by the base voltage V_B. When V_B increases from 0 to 8 V the OLED voltage drop V_{OLED} decreases and the SCLT voltage drop V_{SCLT} increases. Note that the sum of V_{OLED} and V_{SCLT} is always 8 V. The base-emitter bias V_{BE} increases with V_B and the transistor is gradually turned off, corresponding to the off-state in Fig. 6a. The variations of V_{OLED}, V_{SCLT}, V_{BE} as functions of V_B are shown in Table 1. The OLED luminance is shown in both Table 1 and Fig. 8. In the high-luminance state most of the total voltage of 8 V drops across the OLED, whereas in the low-luminance state most of the voltage drops across the SCLT. Note that in the measurement for the independent transistor in Fig. 6 the emitter voltage is fixed when the base voltage is scanned, while in the con-

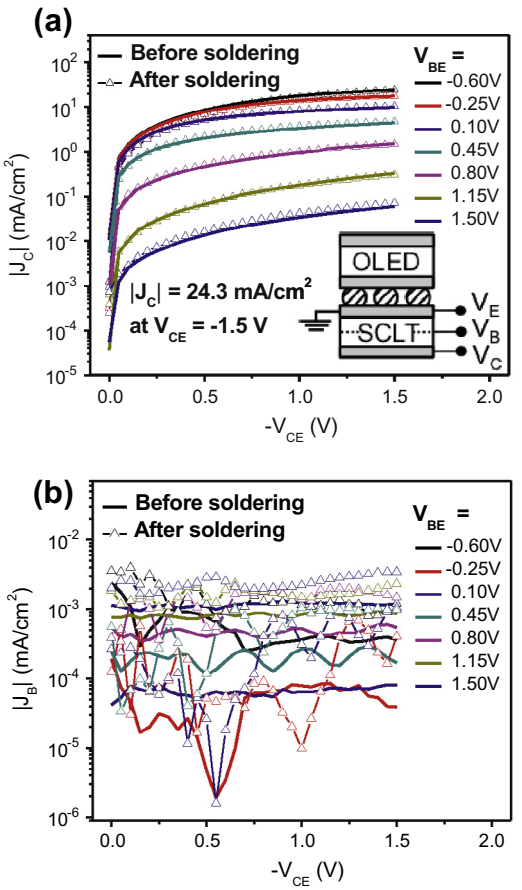

Fig. 6. (a) The output characteristics of SCLT measured before and after soldering by tin balls. The three electrodes are exposed to connect on the device and emitter electrode is connected to the ground. (b) Base leakage current density of SCLT measured before and after soldering.

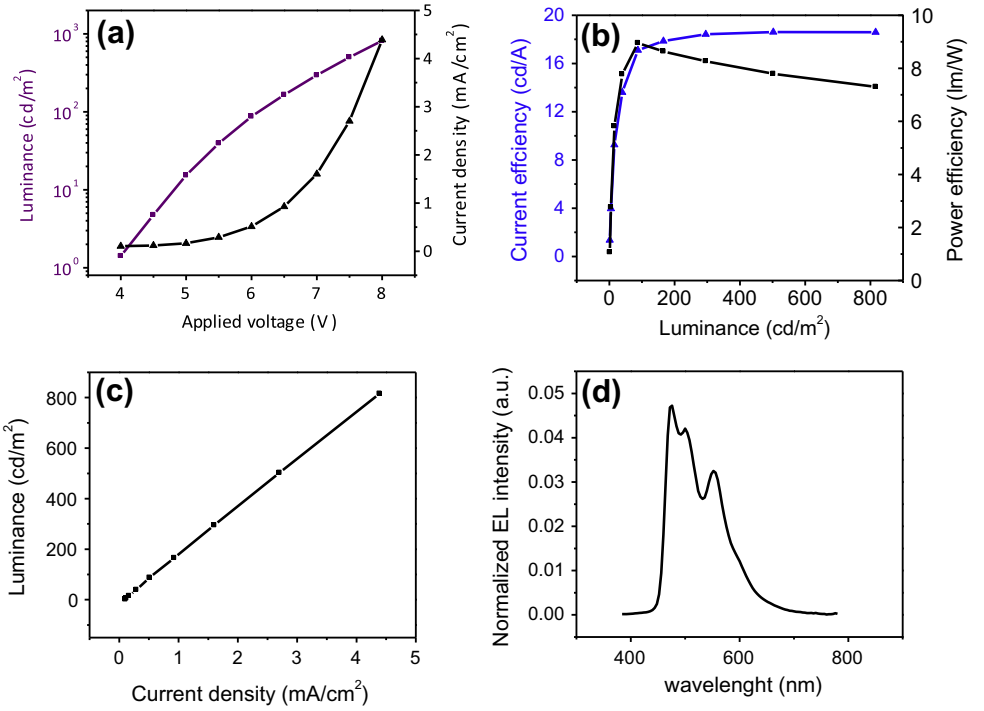

Fig. 7. (a) The luminance and current density versus voltage; (b) efficiency versus luminance; (c) luminance versus current density; (d) the emission spectrum of white emission OLED.

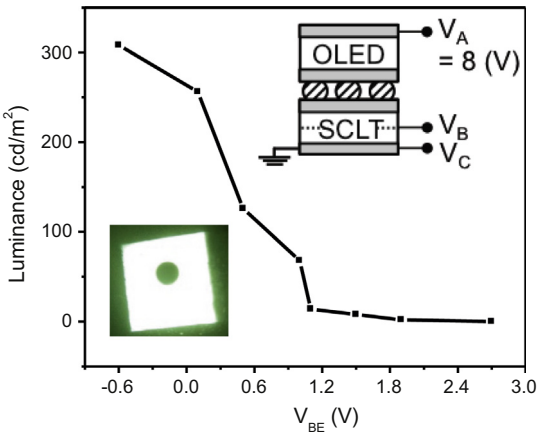

Fig. 8. The luminance of white OLED–V_{BE} curves measured at V_{anode} = 8 V, V_C = 0 V and different V_B and the inset shows the image of white OLED.

nected structure in Fig. 1a the transistor emitter is floating when the base voltage is scanned. In Fig. 8 it is shown that the luminance of the white OLED is turned between dark and 308 cd/cm^2. Higher luminance can be achieved if the total voltage V_A is increase from 8 V to, say, 9 V. Such luminance is close to the requirement of AMOLED display with ideal color filter. In addition to the white OLED, orange OLED with even higher efficiency is soldered with SCLT in a similar fashion. The results are shown in Table 2 and Fig. 9. Luminance of 603 cd/m^2 is achieved at the same voltage range due to higher OLED efficiency. Such single-color OLED can be used in AMOLED without color filter.

Table 1
The variations of V_{OLED}, V_{SCLT}, V_{BE} and luminance of white OLED at various V_B.

White OLED				
V_B (V)	V_{OLED} (V)	V_{SCLT} (V)	V_{BE} (V)	Luminance (cd/m^2)
0	7.4	0.6	−0.6	308
1	7.1	0.9	0.1	256
2	6.5	1.5	0.5	126
3	6.0	2.0	1.0	68
4	5.1	2.9	1.1	12
5	4.5	3.5	1.5	8
6	3.9	4.1	1.9	2
7	3.3	4.3	2.7	0

Table 2
The variations of V_{OLED}, V_{SCLT}, V_{BE} and luminance of the orange OLED at various V_B.

Orange OLED				
V_B (V)	V_{OLED} (V)	V_{SCLT} (V)	V_{BE} (V)	Luminance (cd/m^2)
1	6.9	1.1	−0.1	603
2	6.4	1.6	0.4	425
3	5.6	2.4	0.6	253
4	5.1	2.9	1.1	112
5	4.4	3.6	1.4	41
6	3.8	4.2	1.8	9
7	3.1	4.9	2.1	1
8	2.2	4.8	2.2	0

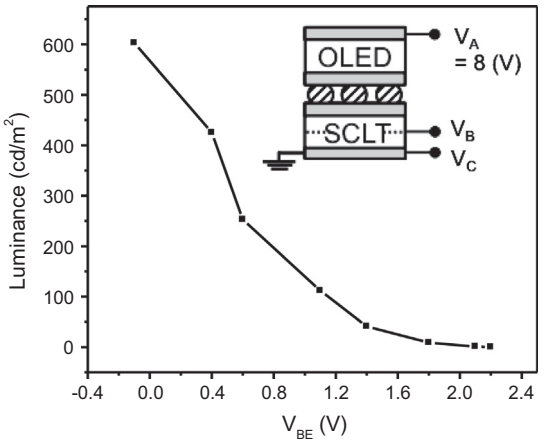

Fig. 9. The luminance of orange OLED–V_{BE} curves measured at V_{anode} = 8 - V, V_C = 0 V and different V_B.

4. Conclusion

Tin ball with diameter of 40 μm are found suitable for the vertical soldering of solution-processed OLED and vertical organic transistor on separated glass substrates. The melting temperature of 139 °C is low enough to ensure that the organic devices are stable and the diameter is large enough to fill any air gap between the substrates. The contact resistance is as low as 10 Ω. The OLED is turned from off to the about 300 cd/m^2 for white emission and 600 cd/m^2 for orange emission, enough for display. Such soldering allows large-area fabrication of OLED array and transistor array on separate glass substrates by solution, followed by lamination in the final phase to complete AMOLED display.

Acknowledgement

This work is supported by the National Science Council of Taiwan and University-Industry Cooperation of E Ink Holdings Inc. under Contract No. 101-2120-M-009-010-CC1, and Ministry of Economic Affairs of Taiwan under Contract No. 101-EC-17-A-07-S1-157. The authors thank the free supply of tin balls from Accurus Scientific Co., Ltd.

References

[1] J.Y. Kwon, K.S. Son, J.S. Jung, T.S. Kim, M.K. Ryu, K.B. Park, B.W. Yoo, J.W. Kim, Y.G. Lee, K.C. Park, S.Y. Lee, J.M. Kim, IEEE Electron Dev. Lett. 29 (2008) 1309.
[2] T. Kamiya, H. Hosono, NPG Asia Mater. 2 (2010) 15.
[3] J.-S. Park, T.-W. Kim, D. Stryakhilev, J.-S. Lee, S.-G. An, Y.-S. Pyo, D.-B. Lee, Y.G. Mo, D.-U. Jin, H.K. Chung, Appl. Phys. Lett. 95 (2009) 013503.
[4] C.-W. Chu, C.-W. Chen, S.-H. Li, E.H.-E. Wu, Y. Yang, Appl. Phys. Lett. 86 (2005) 253503.
[5] Y. Fujisaki, Y. Nakajima, T. Takei, H. Fukagawa, T. Yamamoto, H. Fujikake, IEEE Trans. Electron Dev. 59 (2012) 3442.
[6] C.-W. Han, H.K. Kim, H.S. Pang, S.-H. Pieh, C.J. Sung, H.S. Choi, W.-C. Kim, M.-S. Kim, Y.-H. Tak, J. Display Technol. 5 (2009) 541.
[7] H.-W. Zan, Y.-H. Hsu, H.-F. Meng, C.-H. Huang, Y.-T. Tao, W.-W. Tsai, Appl. Phys. Lett. 101 (2012) 093307.
[8] S.-R. Tseng, H.-F. Meng, K.-C. Lee, S.-F. Horng, Appl. Phys. Lett. 93 (2008) 153308.
[9] C.-Y. Chen, H.-W. Chang, Y.-F. Chang, B.-J. Chang, Y.-S. Lin, P.-S. Jian, H.-C. Yeh, H.-T. Chien, E.-C. Chen, Y.-C. Chao, H.-F. Meng, H.-W. Zan, H.-W. Lin, S.-F. Horng, Y.-J. Cheng, F.-W. Yen, I.-F. Lin, H.-Y. Yang, K.-J. Huang, M.-R. Tseng, J. Appl. Phys. 110 (2011) 094501.
[10] H.-C. Yeh, H.-F. Meng, H.-W. Lin, T.-C. Chao, M.-R. Tseng, H.-W. Zan, Org. Electron. 13 (2012) 914.
[11] Y.-F. Chang, Y.-C. Chiu, H.-C. Yeh, H.-W. Chang, C.-Y. Chen, H.-F. Meng, H.-W. Lin, H.-L. Huang, T.-C. Chao, M.-R. Tseng, H.-W. Zan, S.-F. Horng, Org. Electron. 13 (2012) 2149.
[12] Y.-C. Chao, K.-R. Wang, H.-F. Meng, H.-W. Zan, Y.-H. Hsu, Org. Electron. 13 (2012) 3177.
[13] Y.-C. Chao, H.-K. Tsai, H.-W. Zan, Y.-H. Hsu, H.-F. Meng, S.-F. Horng, Appl. Phys. Lett. 98 (2011) 223303.
[14] W. Ma, C. Yang, X. Gong, K. Lee, A.J. Heeger, Adv. Funct. Mater. 15 (2005) 1617.
[15] S. Cho, K. Lee, J. Yuen, G. Wang, D. Moses, A.J. Heeger, M. Surin, R. Lazzaroni, J. Appl. Phys. 100 (2006) 114503.